© 2022. Published by The Company of Biologists Ltd | Development (2022) 149, dev200788. doi:10.1242/dev.200788

RESEARCH ARTICLE

ISL1/SHH/CXCL12 signaling regulates myogenic cell migration during mouse tongue development

Wei Zhang[1,*], Jiaojiao Yu[1,*], Guoquan Fu[1], Jianying Li[1], Huarong Huang[1], Jing Liu[2], Dongliang Yu[3], Mengsheng Qiu[1] and Feixue Li[1,‡]

ABSTRACT

Migration of myoblasts derived from the occipital somites is essential for tongue morphogenesis. However, the molecular mechanisms of myoblast migration remain elusive. In this study, we report that deletion of *Isl1* in the mouse mandibular epithelium leads to aglossia due to myoblast migration defects. *Isl1* regulates the expression pattern of chemokine ligand 12 (*Cxcl12*) in the first branchial arch through the Shh/Wnt5a cascade. *Cxcl12*$^{+}$ mesenchymal cells in *Isl1*^{ShhCre} embryos were unable to migrate to the distal region, but instead clustered in a relatively small proximal domain of the mandible. CXCL12 serves as a bidirectional cue for myoblasts expressing its receptor CXCR4 in a concentration-dependent manner, attracting *Cxcr4*$^{+}$ myoblast invasion at low concentrations but repelling at high concentrations. The accumulation of *Cxcl12*$^{+}$ mesenchymal cells resulted in high local concentrations of CXCL12, which prevented *Cxcr4*$^{+}$ myoblast invasion. Furthermore, transgenic activation of *Ihh* alleviated defects in tongue development and rescued myoblast migration, confirming the functional involvement of Hedgehog signaling in tongue development. In summary, this study provides the first line of genetic evidence that the ISL1/SHH/CXCL12 axis regulates myoblast migration during tongue development.

KEY WORDS: Isl1, Migration, Myoblast, Mouse

INTRODUCTION

Human congenital tongue malformations that occur during embryogenesis, such as aglossia, microglossia and macroglossia, greatly affect the quality of life of individuals (Cobourne et al., 2019). Tongue development begins with median lingual swelling of the first branchial arch (Kaufman and Bard, 1999). During this stage, the tongue anlage is mainly composed of neural crest cell (NCC)-derived mesenchymal cells. Lateral lingual swellings are then formed on each side of the median tongue bud. Myoblasts from occipital somites migrate along the hypoglossal cord and reach the first arch at about embryonic day (E) 10.5 (Lofqvist and Lindblom, 1994; Parada and Chai, 2015; Parada et al., 2012). Most of the tongue muscle is derived from the occipital myoblasts, whereas the connective tissue and vasculature are derived from NCCs, which originate from the dorsal neural tube (Ziermann et al., 2018). Myoblasts are precisely regulated to migrate to the tongue primordium and proliferate and differentiate, making the tongue a muscular organ. Although epithelial-derived signaling has been found to control tongue morphogenesis, the mechanisms by which epithelial-derived signaling regulates myoblast migration and invasion during tongue development remain unclear (Jeong et al., 2004; Lin et al., 2011).

Multiple signaling pathways and genes have been reported to be involved in the regulation of myoblast migration. *Pax3*, *Gab1* and *Met* have been shown to be essential for the delamination and migration of myogenic progenitor cells to other sites of myogenesis (Amano et al., 2002; Bober et al., 1994; Tajbakhsh and Buckingham, 2000). *Shh*, *Wnt5a* and the CXCL12/CXCR4 axis are also crucial for cell migration and invasion during organogenesis (Jeong et al., 2004; Vasyutina et al., 2005; Yamaguchi et al., 1999). Hedgehog signaling has been shown to be important for the growth and patterning of facial primordium during craniofacial development (Melnick et al., 2005). *Wnt5a* has been shown to regulate directional cell migration and polarity (He et al., 2008; Schlessinger et al., 2007; Witze et al., 2008). The WNT5A pathway underlies the outgrowth of multiple structures in vertebrate embryos, and *Wnt5a* deficiency results in abnormal tongue development (Liu et al., 2012; Yamaguchi et al., 1999). The chemokine *Cxcl12* has been reported to provide directional cues for the migration of many different cell types, such as germ cells, lymphocytes and muscle progenitors (Belmadani et al., 2005; Doitsidou et al., 2002; Ma et al., 1998; Ratajczak et al., 2003; Zou et al., 1998). Previous reports indicate that CXCL12/CXCR4 regulates the migration of both proliferating and terminally differentiated muscle cells (Griffin et al., 2010). However, it remains unclear how these signaling pathways interact between epithelial cells, mesenchymal cells and myoblasts to coordinate tongue development.

Isl1, a member of the LIM homeodomain transcription factor family, has been proven to play crucial roles during left-right body pattern formation, mandible development, anterior teeth formation and cell-type specification in many developmental processes (Li et al., 2017; Pfaff et al., 1996; Yang et al., 2006). We previously found that *Isl1* was exclusively expressed in the distal epithelium of first branchial arch as early as E9.5, and *Isl1* ablation (*Isl1*^{ShhCre}) resulted in defective mandibular outgrowth (Li et al., 2017). In the present study, we report that the *Isl1*^{ShhCre} mice exhibit aglossia due to defects in distal myoblast invasion. We further reveal that the ISL1/SHH/CXCL12 axis regulates distal migration of myoblasts in the first branchial arch during tongue development. Because myoblast migration plays an important role in the development of many organs, the mechanism we identified has important

[1]Zhejiang Key Laboratory of Organ Development and Regeneration, Department of Biological Sciences, Institute of Developmental and Regenerative Biology, College of Life and Environmental Sciences, Hangzhou Normal University, Hangzhou 311121, People's Republic of China. [2]MOE Key Laboratory of Environmental Remediation and Ecosystem Health, Department of Environmental Sciences, College of Environmental and Resource Sciences, Zhejiang University, Hangzhou 310058, People's Republic of China. [3]College of Life Sciences and Medicine, Zhejiang Sci-Tech University, Hangzhou 310018, People's Republic of China.
*These authors contributed equally to this work

‡Author for correspondence (lifx@hznu.edu.cn)

W.Z., 0000-0001-6847-4526; J.Y., 0000-0002-7068-4802; G.F., 0000-0001-5568-6159; J. Li, 0000-0003-1488-8322; H.H., 0000-0002-4363-1190; J. Liu, 0000-0001-8892-036X; D.Y., 0000-0003-3626-0296; M.Q., 0000-0001-6038-3718; F.L., 0000-0001-7234-7191

Handling Editor: James Briscoe
Received 25 March 2022; Accepted 15 September 2022

Development (2022) 149, dev200788. doi:10.1242/dev.200788

implications for understanding the processes of organogenesis and malformation.

RESULTS

Functional Isl1 is required for initiation of tongue

To investigate the potential function of Isl1 in tongue development, we generated mice with an epithelial cell-specific deletion of *Isl1* by crossing *Shh-Cre* with *Isl1*^{fl} mice. Scanning electron microscopy (SEM) analysis demonstrated that the tongue did not develop in *Isl1*^{ShhCre} embryos (100% penetration) (Fig. 1A, Fig. S1). X-gal staining of *Shh*^{Cre}*/R26R* embryos revealed Cre activity in the mandibular arch epithelium at E9.5, E10.5 and E11.5 (Fig. 1B). *Isl1* is expressed in the distal ectoderm of the first branchial arch, but not in the entire mandibular epithelium, as determined by immunofluorescence and the *Isl1-lacZ* knock-in allele (Fig. 1B). Anti-MHC (myosin heavy chain) staining showed that only a stack of residual muscle cells existed in the tongue-forming region of the *Isl1*^{ShhCre} mutant embryos (Fig. 1C). Taste buds were not detected in the *Isl1*^{ShhCre} embryos using an antibody against cytokeratin-8 (CK8, Troma-1; also known as keratin 8, KRT8) (Fig. 1D). Together, these results suggest that an intrinsic function of *Isl1* is required for the tongue formation.

Ablation of Isl1 leads to defective myoblast migration

The absence of the majority of tongue muscle in *Isl1*^{ShhCre} mutant embryos suggests that aglossia may be caused by defective myoblast migration into the tongue primordium. It has been well documented that Pax3 and desmin are expressed in early myogenic precursor cells migrating from the somites into the branchial arch around E10 (Mayo et al., 1992; Tajbakhsh and Buckingham, 2000). Immunofluorescence staining revealed that both Pax3- and desmin-labeled myoblasts reached the floor of the first branchial arch, but did not migrate into the tongue primordium of *Isl1*^{ShhCre} embryos (Fig. 2A, Fig. S2), indicating that in *Isl1*^{ShhCre} mutant mice, myoblasts fail to invade into the tongue mesenchyme after reaching the first branchial arch. The number of Pax3^{+} and desmin^{+} cells in wild type and *Isl1*^{ShhCre} was counted at E10.5 and E11.5. The results showed no significant difference in the number of Pax3^{+} and desmin^{+} cells at E10.5 between control and *Isl1*^{ShhCre} (Fig. 2B,C). However, the number of Pax3^{+} and desmin^{+} cells at E11.5 was reduced in *Isl1*^{ShhCre} compared with wild type (Fig. 2B,C).

We next investigated whether there were differences in myoblast proliferation between *Isl1*^{ShhCre} and wild type. Cyclin D1 immunofluorescence showed that the proliferation of Pax3^{+} myoblasts in *Isl1*^{ShhCre} did not change significantly at E10.5, but decreased significantly at E11.5 (Fig. 2D,E). Consistent with this, 5-bromodeoxyuridine (BrdU) and Ki67 (Mki67) labeling was also reduced in desmin^{+} and Pax3^{+} myoblasts in *Isl1*^{ShhCre} embryos at E11.5 (Fig. 2D,F,G). Terminal deoxynucleotidyl transferase dUTP nick end labeling (TUNEL) analysis revealed no significant changes in apoptosis in *Isl1*^{ShhCre} embryos at E11.5 (Fig. 2H). Myoblast differentiation was examined by expression of the myoblast differentiation marker myogenin (Myog) and no apparent differences were detected between wild-type and *Isl1*^{ShhCre} embryos (Fig. 2I). These results demonstrate that in *Isl1*^{ShhCre} mutant embryos myoblast proliferation is reduced after reaching the first branchial arch, but their differentiation and survival are not affected.

Loss of Isl1 results in decreased expression of Shh in distal ectoderm of the first branchial arch

It has been reported that the Hedgehog signaling in NCC-derived mesenchyme may be involved in the transmission of information from epithelial cells to myogenic progenitor cells (Parada and Chai, 2015). We propose that *Isl1* may regulate tongue development by affecting *Shh* expression in epithelial cells. Real-time PCR results showed that the expression of *Shh* was significantly downregulated in the mandible of *Isl1*^{ShhCre} embryos at E10.5 (Fig. 3A). *Ptch1*, *Gli1*, *Foxd1*, *Foxd2*, *Foxf1* and *Foxf2* are all reported to be the target genes of Hedgehog signaling in cranial NCCs (Jeong et al., 2004).

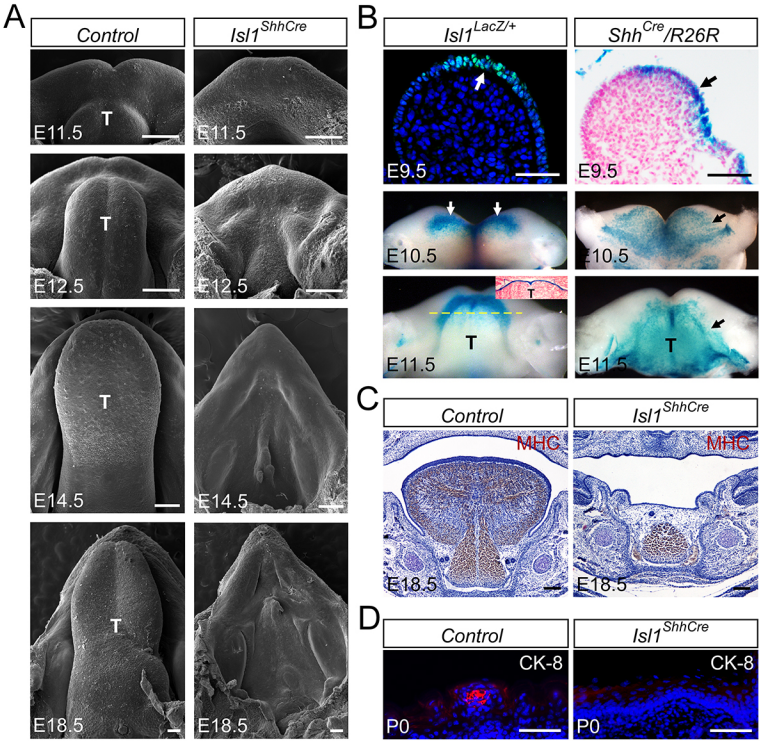

Fig. 1. *Isl1* is required for mouse tongue morphogenesis. (A) SEM showing the early development of the mouse tongue in *Shh*^{Cre} (control) and *Isl1*^{ShhCre} mice (*n*=4). (B) Left: Immunofluorescence staining with ISL1 antibody on sagittal sections of E9.5 mandibles in wild type (white arrow) mice (*n*=4). X-Gal staining showing Isl1 expression in *Isl1*$^{lacZ/+}$ knock-in mice at E10.5 and E11.5 (white arrows) (*n*=5). Yellow dashed line indicates approximate section levels crossing the mandible. Inset shows Hematoxylin and Eosin staining on coronal sections. Right: X-Gal staining showing Shh-Cre activity in E9.5, E10.5 and E11.5 *Shh*^{Cre}*/R26R* mandibular arch (black arrows) (*n*=4). (C) Immunohistochemistry with MHC antibody on coronal sections of E18.5 mandibles in *Shh*^{Cre} (control) and *Isl1*^{ShhCre} mice (*n*=4). (D) Immunofluorescence staining with CK-8 antibody on coronal sections of postnatal day 0 (P0) tongues in *Shh*^{Cre} (control) and *Isl1*^{ShhCre} mice (*n*=4). T, tongue. Scale bars: 200 µm (A,C); 100 µm (B); 20 µm (D).

Development (2022) 149, dev200788. doi:10.1242/dev.200788

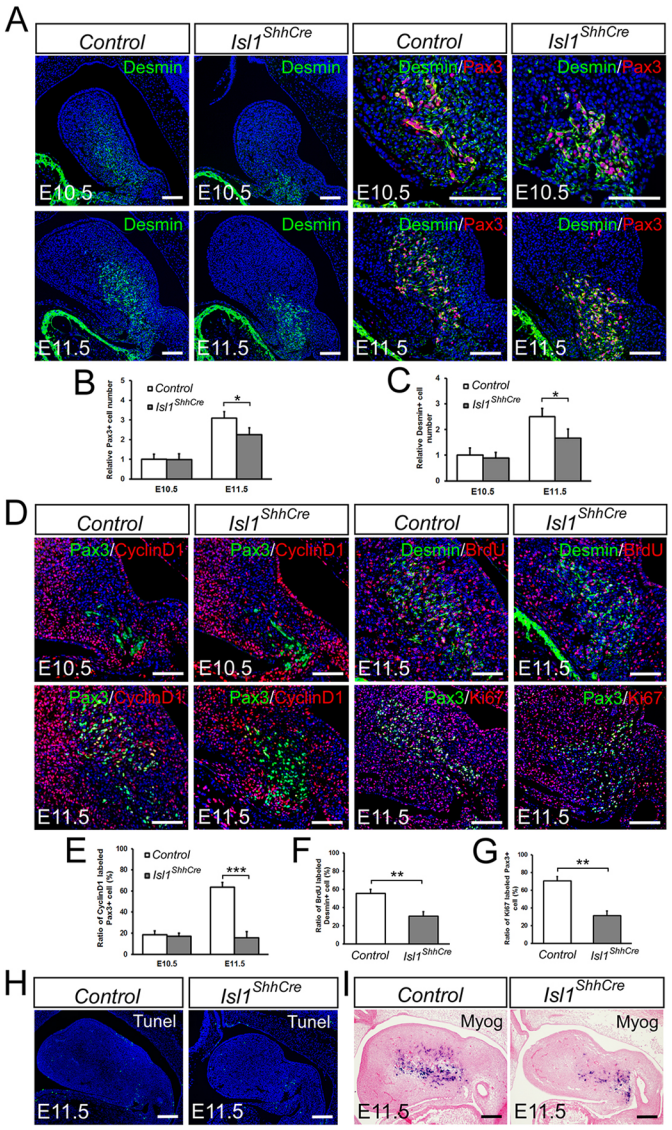

Fig. 2. Deletion of *Isl1* in epithelial cells leads to a defect in myoblast cell invasion and proliferation. (A) Double immunofluorescence staining with desmin and Pax3 antibodies on sagittal sections of E10.5 and E11.5 mandibles (n=5). (B) Quantification of the total number of Pax3$^+$ cells in *Shh*^{Cre} (control) and *Isl1*^{ShhCre} mice. (C) Quantification of the total number of desmin$^+$ cells in *Shh*^{Cre} (control) and *Isl1*^{ShhCre} mice. (D) Double immunofluorescence staining with Pax3 and cyclin D1, desmin and BrdU, Pax3 and Ki67 on sagittal sections of E10.5 and E11.5 mandibles (n=5). (E) Quantification of cyclin D1$^+$ Pax3$^+$ cells versus total Pax3$^+$ cells in *Shh*^{Cre} (control) and *Isl1*^{ShhCre} mice. (F) Quantification of BrdU$^+$ desmin$^+$ cells versus total desmin$^+$ cells in *Shh*^{Cre} (control) and *Isl1*^{ShhCre} mice. (G) Quantification of Ki67$^+$ positive Pax3$^+$ cells versus total Pax3$^+$ cells in *Shh*^{Cre} (control) and *Isl1*^{ShhCre} mice. (H) TUNEL staining on sagittal sections of E11.5 mandibles in *Shh*^{Cre} (control) and *Isl1*^{ShhCre} mice (n=4). (I) *In situ* hybridization of Myog on sagittal sections of E11.5 mandibles in *Shh*^{Cre} (control) and *Isl1*^{ShhCre} mice (n=4). Error bars represent s.d. (n=3-6 samples). *P<0.05; **P<0.01; ***P<0.001 (unpaired, two-tailed Student's t-test). Scale bars: 200 µm.

Quantitative RT-PCR analysis showed that the expression of *Ptch1*, *Gli1*, *Foxd1*, *Foxd2*, *Foxf1* and *Foxf2* was significantly decreased in the first branchial arch of *Isl1*^{ShhCre} mutants (Fig. 3A, Fig. S3). Whole-mount *in situ* hybridization results demonstrated that the expression of *Shh* was much reduced in the distal epithelium of the

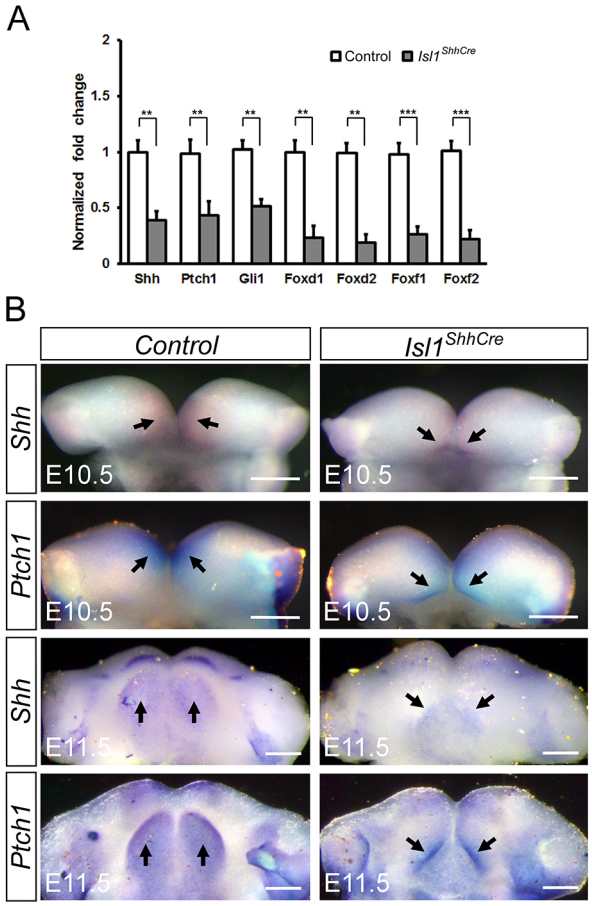

Fig. 3. Loss of *Isl1* leads to downregulation of *Shh* in the distal ectoderm of the *Isl1*^{ShhCre} mandible. (A) Quantitative RT-PCR of *Shh*, *Ptch1*, *Gli1*, *Foxd1*, *Foxd2*, *Foxf1* and *Foxf2* independently in derived mandibular arch RNA samples (n=3-6 samples). (B) Whole-mount *in situ* hybridization showing the expression of *Shh* and *Ptch1* in *Shh*^{Cre} (control) and the *Isl1*^{ShhCre} mutant at E10.5 and E11.5 (n=6). **P<0.01; ***P<0.001 (unpaired, two-tailed Student's t-test). Scale bars: 200 µm.

first branchial arch (Figs 3B and 4). The expression of *Ptch1* was also downregulated in the distal region of the mandible of the *Isl1*^{ShhCre} mutant (Figs 3B and 4). These results indicate that *Isl1* in the distal ectoderm regulates *Shh* expression in anterior tongue epithelial cells.

Downregulation of the Shh signaling pathway leads to an abnormal expression pattern of *Cxcl12* in the first branchial arch

Previous studies have shown that the chemokine CXCL12 provides directional cues for migrating CXCR4-expressing muscle progenitors in the limbs (Vasyutina et al., 2005). In the developing first branchial arch, CXCL12 is expressed in the mesenchymal cells, and its receptor CXCR4 is expressed in the muscle progenitors (Vasyutina et al., 2005). The co-expression of CXCR4 and desmin in myoblasts was confirmed by immunofluorescence (Fig. S4). At E10.5, expression of *Cxcl12* mRNA but not *Cxcr4* mRNA was detected at the base of the tongue primordium, suggesting that *Cxcl12*-expressing mesenchymal cells populate the tongue anlage prior to myoblast invasion (Fig. 4C-D′). At E11.5, the expression domains of *Cxcl12* and *Cxcr4* similarly extended into the middle region of the tongue primordia in wild-type embryos (Fig. 4G,H). In contrast, there was no colocalization

Development (2022) 149, dev200788. doi:10.1242/dev.200788

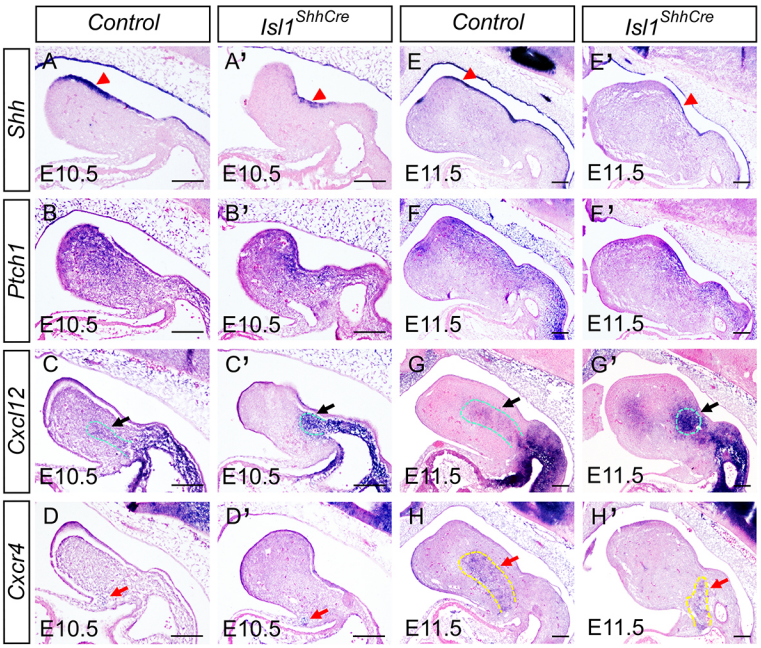

Fig. 4. Comparison of *Shh* and *Cxcl12* expression in *Isl1*^{ShhCre} mandible. *In situ* hybridization of *Shh* (A,A′,E,E′, red arrowheads), *Ptch1* (B,B′,F,F′), *Cxcl12* (C,C′,G,G′, black arrows) and *Cxcr4* (D,D′,H,H′, red arrows) on sagittal sections of E10.5 (A-D′) and E11.5 (E-H′) mandibles in *Shh*^{Cre} (control) and *Isl1*^{ShhCre} mice (*n*=5). Green dashed lines show the expression domain of *Cxcl12* and yellow dashed lines show the expression domain of *Cxcr4*. Scale bars: 200 µm.

of *Cxcl12* and *Cxcr4* expression in *Isl1*^{ShhCre} (Fig. 4G′,H′), suggesting that Cxcr4^{+} myoblasts did not reach the *Cxcl12* expression domain. In addition, the expression region of *Cxcl12* in the first branchial arch of the *Isl1*^{ShhCre} mutant did not extend as far, and its expression in the *Isl1*^{ShhCre} mutant was much higher than that in the wild type (Fig. 4C,C′,G,G′). *Cxcl12* expression was only detected in the proximal mesenchyme below the *Shh*-expressing epithelium, suggesting that *Shh* expression in the mandibular epithelium may determine the region of *Cxcl12* expression (Fig. 4A-C′,E-G′). Thus, we hypothesize that aberrant expression patterns of *Shh* and *Cxcl12* in the first branchial arch lead to the migration defect of *Cxcr4*$^{+}$ myoblasts.

Canonical Hedgehog pathway is essential for the expression pattern of *Cxcl12* and invasion of myoblasts in the first branchial arch

To determine whether Hedgehog signaling regulates myoblast migration, we generated mice with an NCC-specific deletion of *Smo* by crossing *Wnt1-Cre* with *Smo*^{fl} mice. Similar to the phenotype of *Isl1*^{ShhCre}, the tongue was absent in *Smo*^{Wnt1Cre} embryos as a result of myoblast migration defects (100% penetration) (Fig. 5A,B). There was no expression of *Ptch1* in the first branchial arch and adjacent pharyngeal arch of *Smo*^{Wnt1Cre} mice, indicating that the activity of the Hedgehog pathway is blocked (Fig. 5C). *In situ* hybridization revealed that *Cxcl12* expression was absent in the first

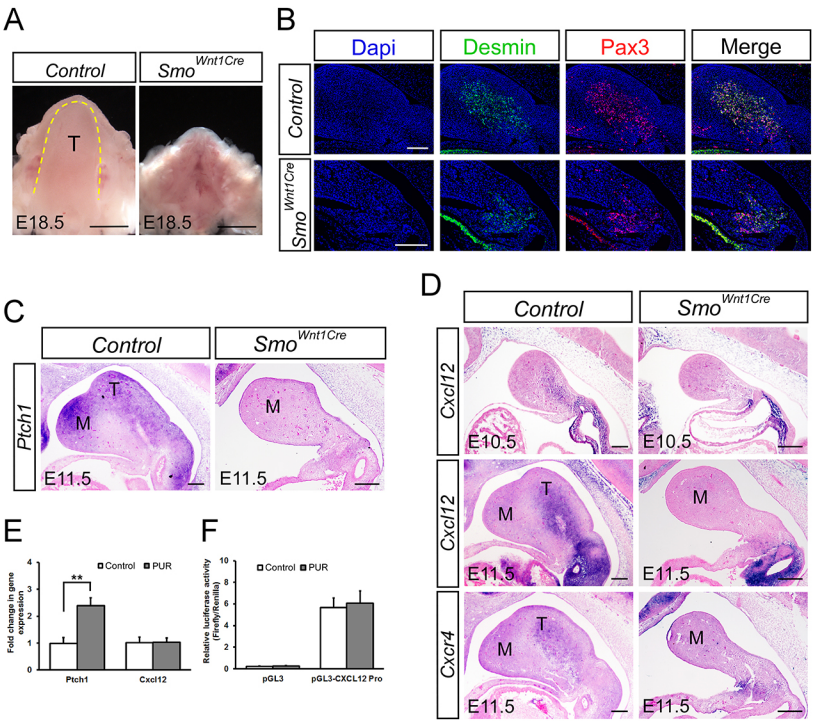

Fig. 5. Deletion of *Smo* in NCCs leads to a defect in *Cxcl12* expression and myoblast migration. (A) Morphological analysis of E18.5 *Wnt1*^{Cre} (control) and *Smo*^{Wnt1Cre} mouse tongues (*n*=4). Dashed line indicates tongue. (B) Double immunofluorescence staining for desmin (green) and Pax3 (red) on sagittal sections of E11.5 *Wnt1*^{Cre} (control) and *Smo*^{Wnt1Cre} mandibles (*n*=5). DAPI was used as counterstain. (C) *In situ* hybridization of *Ptch1* on sagittal sections of E11.5 *Wnt1*^{Cre} (control) and *Smo*^{Wnt1Cre} mandibles (*n*=4). (D) *In situ* hybridization of *Cxcl12* and *Cxcr4* on sagittal sections of E10.5 and E11.5 *Wnt1*^{Cre} (control) and *Smo*^{Wnt1Cre} mandibles (*n*=4). (E) Quantitative RT-PCR demonstrates transcription of *Ptch1* and *Cxcl12* in primary mesenchymal cell cultures (*n*=5). Purmorphamine (PUR) (1 µM) was used to active the canonical Hedgehog pathway. ***P*<0.01 (unpaired, two-tailed Student's *t*-test). (F) Luciferase activity of pGL3 empty vector (control) and pGL3-CXCL12 promoter vector (pGL3-CXCL12 Pro) after PUR (1 µM) treatment in primary cell cultures (*n*=5). M, mandible; T, tongue. Scale bars: 1 mm (A); 200 µm (B-D).

Development (2022) 149, dev200788. doi:10.1242/dev.200788

branchial arch at E10.5 and E11.5, but the expression of *Cxcl12* in the adjacent pharyngeal arch was not affected (Fig. 5D), indicating that only the expression of *Cxcl12* in the first branchial arch was dependent on activation of the canonical Hedgehog pathway in NCCs. The results of immunofluorescence and *in situ* hybridization showed that desmin^{+}, Pax3^{+} and *Cxcr4*$^{+}$ myoblasts did not migrate into the tongue anlage in *Smo*^{Wnt1Cre} embryos (Fig. 5B,D), suggesting that activation of canonical Hedgehog pathway in NCCs is required for *Cxcl12* expression in the first branchial arch and for myoblast invasion. There was no significant difference in the number of *Cxcl12*$^{+}$ mesenchymal cells between wild type and *Isl1*^{ShhCre} at E9.5 and E10.5 (Fig. S5A-D). Our real-time PCR results also showed no significant difference in the expression of *Cxcl12* mRNA between *Isl1*^{ShhCre} and wild type in the first branchial arch at E10.5 (Fig. S5E). We further investigated the effect of Hedgehog signaling on expression of *Cxcl12* at the transcriptional level. The 2 kb promoter of *Cxcl12* was cloned into the pGL3 vector (pGL3-CXCL12 Pro). Purmorphamine (PUR), an agonist of the Smo receptor, had no effect on *Cxcl12* mRNA expression and *Cxcl12* promoter activity (Fig. 5E,F). Therefore, we hypothesize that *Shh* regulates the expression pattern of *Cxcl12* by affecting the migration of *Cxcl12*-expressing mesenchymal cells in the first branchial arch.

Shh regulates the migration of *Cxcl12*$^{+}$ mesenchymal cells through *Wnt5a*

Considering that *Wnt5a* affects cell migration and can alter outgrowth of many structures, including the tongue (He et al., 2008; Liu et al., 2012; Schlessinger et al., 2007; Witze et al., 2008; Yamaguchi et al., 1999), it is possible that the reduction of *Shh* expression limits the migration of *Cxcl12*$^{+}$ mesenchymal cells through *Wnt5a*. Consistent with this idea, *Wnt5a* expression was detected in the proximal domain below the *Shh*-expressing epithelium in *Isl1*^{ShhCre} embryos (Fig. 6A). The expression of *Wnt5a* was also significantly reduced in *Smo*^{Wnt1Cre} embryos (Fig. 6B). More importantly, *Wnt5a* expression was strongly induced by SHH-saturated beads (Fig. 6C), or purified recombinant SHH protein in mandible explant culture (Fig. 6D). These results suggest that expression of *Wnt5a* in the tongue is regulated by *Shh*. In addition, WNT5A-saturated beads were able to attract *Cxcl12*$^{+}$ cells to migrate from the adjacent pharyngeal arch in wild-type embryos (Fig. 6F). Defects in *Cxcl12*$^{+}$ cell migration could also be rescued by WNT5A beads in *Isl1*^{ShhCre} embryos (Fig. 6G). Moreover, the expression of *Cxcl12* was not altered after WNT5A treatment (Fig. 6E). Overall, these results suggest that the migration of *Cxcl12*$^{+}$ mesenchymal cells is regulated by the SHH/WNT5A cascade, and the abnormal migration and accumulation of *Cxcl12*$^{+}$ mesenchymal cells in *Isl1*^{ShhCre} is due to changes in the expression patterns of *Shh* and *Wnt5a*.

CXCL12 is a bi-directional cue for myoblast cells

Mandible explant cultures were used to determine whether the chemotaxis of myoblasts changes with the concentration of CXCL12. Low concentration (100 ng/µl) of CXCL12 protein-saturated beads obviously attracted desmin^{+} myoblasts to the protein beads (Fig. 7A). By contrast, desmin^{+} myoblasts aggregated into circular bands at a certain distance from beads saturated with high concentration (500 ng/µl) of CXCL12 protein (Fig. 7A), indicating that a high concentration of CXCL12 protein can attract myoblasts to aggregate nearby, but prevent myoblasts from approaching. CXCL12 protein diffuses from the beads to the surroundings, forming a concentration gradient from high to low. When CXCL12 reaches a certain concentration in the circular band, the attraction and repulsion effect of CXCL12 on myoblasts reaches a balance.

We hypothesized that the migration of *Cxcl12*$^{+}$ cells is crucial for establishing a concentration gradient of CXCL12, which attracts myoblast migration during tongue development. CXCL12 beads were implanted in *Isl1*^{ShhCre} mandibles to investigate whether myoblasts can be repelled or attracted into the tongue primordium despite the lack of *Cxcl12*$^{+}$ cell migration (Fig. 7B). The results showed that high (500 ng/µl) and low (100 ng/µl) concentrations of CXCL12 protein-saturated beads repelled or attracted desmin^{+} myoblasts migration, respectively (Fig. 7B). This suggests that myoblast migration is regulated by CXCL12 protein concentration and that the migration of *Cxcl12*$^{+}$ mesenchymal cells secreting CXCL12 protein is crucial for myoblast migration.

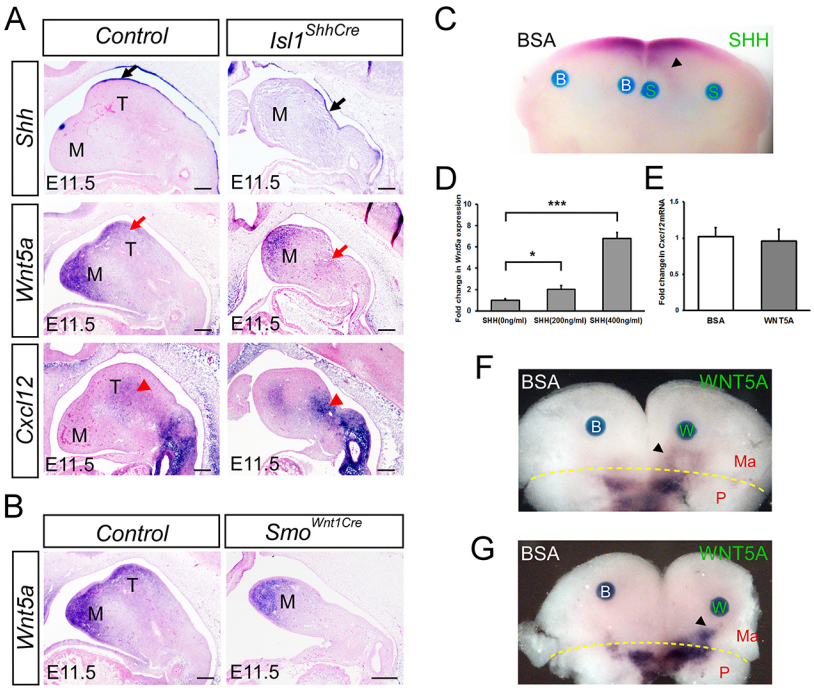

Fig. 6. Shh regulates the migration of *Cxcl12*$^{+}$ cells through *Wnt5a*. (A) *In situ* hybridization of *Shh* (black arrows), *Wnt5a* (red arrows) and *Cxcl12* (red arrowheads) on sagittal sections of E11.5 mandibles in *Shh*^{Cre} (control) and *Isl1*^{ShhCre} mice (n=4). (B) *In situ* hybridization of *Wnt5a* on sagittal sections of E11.5 mandibles in *Shh*^{Cre} (control) and *Smo*^{Wnt1Cre} mice (n=4). (C) Effect of SHH protein on *Wnt5a* expression in mandibular culture (n=5). An SHH-saturated (1 µg/µl), but not bovine serum albumin (BSA)-saturated, bead induces the expression of *Wnt5a* (arrowhead). (D) Quantitative RT-PCR demonstrates transcription of *Wnt5a* in mandibular organ cultures after SHH protein treatment. Error bars represent s.d. (n=3-6 samples). *P<0.05; ***P<0.001 (unpaired, two-tailed Student's t-test). (E) Quantitative RT-PCR showing expression of *Cxcl12* in mandibular organ cultures after WNT5A protein treatment. (F,G) Effect of WNT5A protein on CXCL12-expressing cells migration in wild-type (F) (n=4) and *Isl1*^{ShhCre} (G) (n=3) mandibles. A WNT5A-saturated (0.5 µg/µl), but not BSA-saturated, bead attracts the migration of CXCL12 positive cells (arrowheads). The yellow line shows the boundary between the mandibular arch (Ma) and adjacent pharyngeal arch (P). B, BSA; S, Shh; W, WNT5A; M, mandible; T, tongue. Scale bars: 200 µm.

Development (2022) 149, dev200788. doi:10.1242/dev.200788

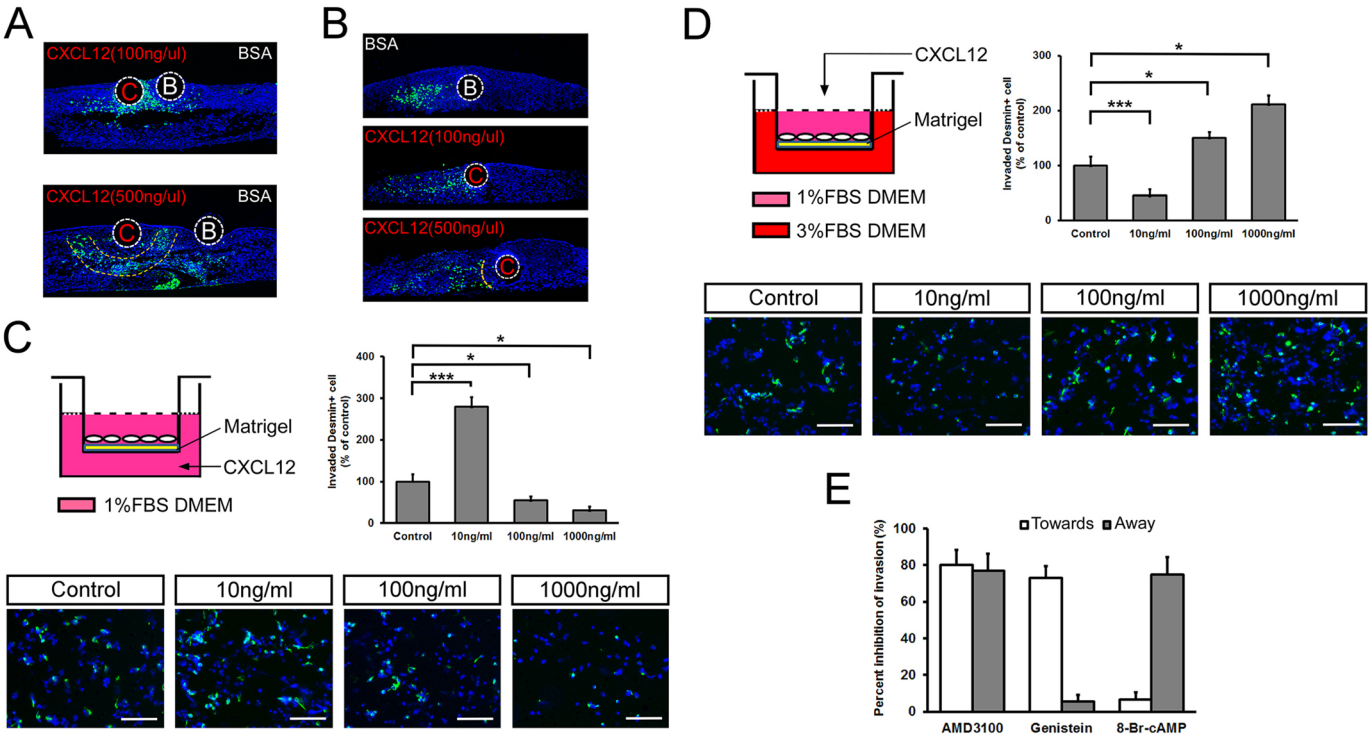

Fig. 7. CXCL12 has a concentration-dependent bi-functional chemotactic effect on myoblasts. (A,B) Immunostaining of desmin in mandible explants from E11 wild-type (n=4) (A) and *Isl1*^{ShhCre} (n=4) (B) mice cultured with BSA control or CXCL12 beads. CXCL12 attracts the migration of desmin$^+$ myoblasts at 100 ng/µl, but repels them at 500 ng/µl. Curved dashed lines delineate the distribution of desmin$^+$ cells. B, BSA; C, CXCL12. (C) For the chemotaxis assay, primary cells isolated from E11 tongue tissue of wild-type embryos were added to the upper chamber (2×10^5 per well), and CXCL12 was added to the lower chamber at varying concentrations (0, 10, 100 and 1000 ng/ml). The figure shows the invasion of desmin$^+$ cells at different concentrations of CXCL12. (D) For the competitive chemotaxis assay, CXCL12 (0, 10, 100 and 1000 ng/ml) was mixed with isolated primary cells (1×10^5 per well) plated to the upper chamber in media containing 1% (v/v) FBS. Media containing 3% (v/v) FBS was added to the lower chamber. The cells on the upper surface of the membrane were removed using a cotton swab after 24 h. The membranes were cut from inserts and mounted onto glass slides for immunofluorescence staining. Desmin antibody was used to label myoblasts. The figure shows the invasion of desmin$^+$ cells at different concentrations of CXCL12. (E) Movement towards and away from CXCL12 has different sensitivities to inhibitors and cyclic nucleotide agonists. Primary cells were incubated with the CXCR4 inhibitor AMD3100, the tyrosine kinase inhibitor genistein and the membrane-permeable cAMP agonist 8-BrcAMP, and then were added to the chemotaxis assay. The percentage inhibition of movement of desmin$^+$ myoblasts towards or away from 10 ng/ml and 1 mg/ml SDF-1 was determined. Error bars represent s.d. (n=3-6 samples). *P<0.01; ***P<0.001 (unpaired, two-tailed Student's t-test). Scale bars: 200 µm.

Primary cultures of a mixture of mesenchymal cells and myoblasts isolated from the E11 tongue tissue of wild-type embryos were used to evaluate the chemotaxis of CXCL12. The inserts were coated with Matrigel matrix to mimic the *in vivo* environment. When CXCL12 was added to the lower chamber, the chemotactic attraction activities of CXCL12 on desmin$^+$ myoblast cells were observed with a maximum effect at 10 ng/ml (Fig. 7C). At this concentration, the number of desmin$^+$ cells that transmigrated to the lower chamber was more than three times that of control. The movement of desmin$^+$ myoblasts towards CXCL12 dramatically decreased when the CXCL12 concentration was increased to 1000 ng/ml (Fig. 7C). The number of desmin$^+$ cells that transmigrated was less than half that of the control, suggesting that desmin$^+$ myoblasts would move away from CXCL12. These results confirmed that CXCL12 attracts *Cxcr4*$^+$ myoblasts at low concentrations but repels them at high concentrations.

A competitive chemotaxis assay was also used to confirm the bidirectional effect of CXCL12 on myoblast invasion. When CXCL12 was added to the upper chamber, the movement of desmin$^+$ myoblasts away from CXCL12 reached a maximum at 1000 ng/ml, with about twice as many desmin$^+$ cells transmigrating than in the control (Fig. 7D). Conversely, when the CXCL12 concentration was decreased to 10 ng/ml the number of desmin$^+$ cells that transmigrated was less than half of the number transmigrating in control. These data illustrate a concentration-dependent bidirectional movement of myoblasts in response to CXCL12 (Fig. 7D). The direction of myoblast invasion depends on the concentration of CXCL12, suggesting that CXCL12 functions as an attractant for *Cxcr4*$^+$ myoblasts in normal developing tongue tissue, but abnormally high levels of CXCL12 in the tongue primordia of *Isl1*^{ShhCre} mutants prevent myoblast invasion.

Treatment with the selective CXCR4 inhibitor AMD3100 resulted in inhibition of myoblast movement in response to CXCL12 in both directions (away and towards) (Fig. 7E). It has been reported that CXCL12 can induce activation of tyrosine kinase and inhibition of cAMP (Chalasani et al., 2003; Ganju et al., 1998; Xu et al., 2010). Pre-incubation of myoblasts with the tyrosine kinase inhibitor genistein only inhibited movement towards CXCL12, but had no effect on movement away from CXCL12. In contrast, the membrane-permeable cAMP agonist 8-Br-cAMP blocked movement away from CXCL12, but had no effect on movement towards the chemokine (Fig. 7E). These data indicate that the attraction and repulsion of myoblasts by CXCL12 are mediated by distinct signaling pathways.

Defective tongue development is partially rescued by activation of the Hedgehog pathway

To test further the hypothesis that *Isl1* regulates tongue development through Hedgehog signaling, we next examined whether *Ihh* could

Development (2022) 149, dev200788. doi:10.1242/dev.200788

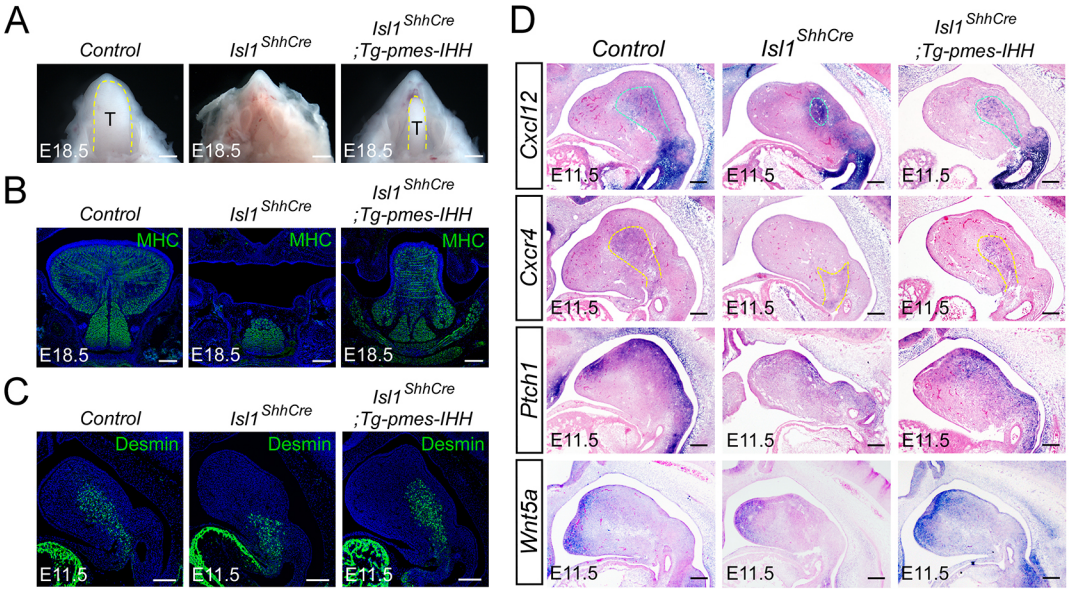

Fig. 8. Reactivation of Hedgehog signaling rescues tongue development in *Isl1*^{ShhCre} mutant embryos. (A) Morphological analysis of E18.5 *Shh*^{Cre} (*n*=4) (control), *Isl1*^{ShhCre} and *Isl1*^{shhCre}; Tg-*pmes-Ihh* mice tongues (*n*=5). Dashed line indicates tongue. (B) MHC immunofluorescence staining on coronal sections of E18.5 mandibles in *Shh*^{Cre} (control) and *Isl1*^{ShhCre} mice (*n*=5). (C) Immunofluorescence analysis for desmin (green) on sagittal sections of E11.5 *Shh*^{Cre} (control), *Isl1*^{ShhCre} and *Isl1*^{ShhCre}; Tg-*pmes-Ihh* mandibles (*n*=5). (D) *In situ* hybridization showing the expression pattern restoration of *Cxcl12*, *Cxcr4*, *Ptch1* and *Wnt5a* in the *Isl1*^{ShhCre}; Tg-*pmes-Ihh* mandibular arch (*n*=4). Green dashed lines show the expression pattern of *Cxcl12* and yellow dashed lines show the expression domain of *Cxcr4*. T, tongue. Scale bars: 1 mm (A); 200 µm (B-D).

rescue the defective tongue morphogenesis in *Isl1*^{ShhCre}. We took a transgenic gain-of function approach by overexpressing *Ihh* in the mandibular epithelium using a conditional Ihh transgenic allele (Tg-*pmes-Ihh*), as *Ihh* and *Shh* could activate the same canonical Hedgehog signaling pathway (Jenkins, 2009). As expected, transgenic *Ihh* did indeed alleviate the defect of aglossia, and the *Isl1*^{ShhCre}; Tg-*pmes-Ihh* allele displayed microglossia (Fig. 8A,B). The invasion of myoblasts (Pax3^{+} and desmin^{+}) was rescued after expression of *Ihh* (Fig. 8C, Fig. S6) as was the proliferation of myoblasts (Fig. S6). Moreover, *Ptch1* expression was induced in the mesenchyme of the tongue, indicating activation of Hedgehog signaling (Fig. 8D). The colocalization of *Cxcl12*$^{+}$ and *Cxcr4*$^{+}$ cells was restored by expression of transgenic *Ihh* (Fig. 8D). The expression of *Wnt5a* was also restored in *Isl1*^{ShhCre}; Tg-*pmes-Ihh* embryos (Fig. 8D). Although expression of *Ihh* was insufficient to fully rescue the tongue development defect, the genetic integration of Hedgehog signaling was evident. The signaling cascade model controlling myoblasts invasion during tongue morphogenesis is illustrated in Fig. 9.

DISCUSSION

Although the tongue is an extremely important organ in mammals, the molecular mechanisms of tongue morphogenesis remain poorly understood owing to its complex anatomy and cell origins (Noden and Francis-West, 2006). In this study, we demonstrate that the transcription factor *Isl1* is required for tongue development, as deletion of *Isl1* in the epithelium of the first branchial arch results in defects in myoblast invasion.

Tongue myogenic progenitors originate from the occipital somites and migrate along hypoglossal cord to the tongue primordium at about E10.5 (Mackenzie et al., 1998). Both desmin and Pax3 mark the early myogenic precursor cells that migrate from the somite to the branchial arch (Mayo et al., 1992; Tajbakhsh and Buckingham, 2000). In this study, desmin^{+} and Pax3^{+} myogenic cells were observed in the floor of first branchial arch at E10.5 in both wild-type and *Isl1*^{ShhCre} embryos. However, the myogenic cells did not invade into the tongue primordium after they arrived the first branchial arch of *Isl1*^{ShhCre} embryos. It has been reported that NCCs initiate tongue development and populate the tongue primordium prior to the invasion of myogenic progenitors (Chai and Maxson, 2006). Therefore, we hypothesized that ablation of *Isl1* in epithelial cells results in a microenvironment in the tongue primordium that is unconducive to muscle cell invasion.

The chemokine receptor CXCR4 and its ligand CXCL12 provide guidance for many different cell types, such as lymphocytes, germ cells, hematopoietic cells and muscle progenitor cells (Belmadani et al., 2005; Doitsidou et al., 2002; Ma et al., 1998; Ratajczak et al., 2003; Zou et al., 1998). All of these different cell types are simultaneously and accurately guided by CXCL12 to different targets, suggesting tight control over the spatial and temporal distribution of CXCL12 (Lewellis and Knaut, 2012). CXCL12 is expressed in the mesenchyme of limb bud and the first branchial arch, and its receptor CXCR4 is expressed in migrating muscle progenitors (Vasyutina et al., 2005). However, it has been reported that CXCR4-positive muscle progenitor cells did not migrate to the center of limb buds with high CXCL12 expression, but instead localized to the surrounding area (Vasyutina et al., 2005). This strongly suggests that the expression level of CXCL12 may regulate the distribution of muscle progenitors. Here, we found abnormally high *Cxcl12* mRNA expression in the mandibular arch of *Isl1*^{ShhCre} embryos. We propose that this higher CXCL12 expression in the presumptive tongue primordium leads to defects in myoblast invasion. Consistent with this concept, our chemotaxis assays demonstrate that CXCL12 has a concentration-dependent bi-functional effect on myoblasts invasion, attracting *Cxcr4*$^{+}$ myoblast invasion at low concentrations but repelling at high concentrations. The invasion and distribution of *Cxcr4*$^{+}$ myoblasts during tongue and limb development may be precisely regulated by the intensity of CXCL12 expression. This is the first study to find that CXCL12 has a bi-functional effect on myoblast invasion.

Development (2022) 149, dev200788. doi:10.1242/dev.200788

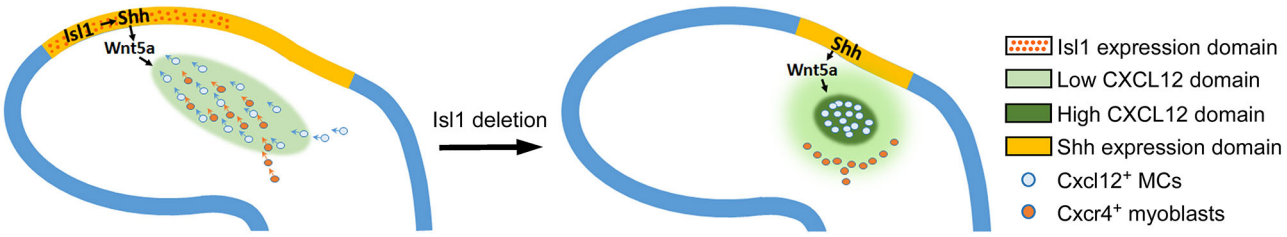

Fig. 9. Model of the signaling cascade governing distal myoblast cell invasion in the tongue. In wild-type embryos, *Shh* is expressed in the mandible distal epithelium cells, and WNT5A induces the migration of *Cxcl12*-positive cells into the distal mesenchyme domain. *Cxcr4*-positive myoblasts are attracted by CXCL12 and invade into the presumptive tongue primordium. In *Isl1*^{ShhCre} mutant embryos, *Shh* expression in the mandible distal epithelium cells is missing. *Cxcl12*-positive cells accumulate in the proximal mesenchyme, which leads to high CXCL12 concentration in this domain. The chemotactic repelling effect of high concentrations of CXCL12 leads to an invasion defect of *Cxcr4*-positive myoblasts. MCs, mesenchymal cells.

Consistent with our observations, a previous study reported a similar bi-functional effect of CXCL12 in T-cell migration (Poznansky et al., 2000).

How might *Isl1* in the distal ectoderm alter the expression pattern of *Cxcl12* in the mesenchyme? Hedgehog signaling plays an important role in coordinating reciprocal epithelial-mesenchymal interactions during organogenesis. The expression domain of *Shh* in the epithelium seems to determine where the tongue develops (Jeong et al., 2004). Here, we demonstrate that *Shh* is regulated by *Isl1* in oral ectoderm-derived lingual epithelium. We propose that downregulation of *Shh* leads to defects in myoblast migration during tongue development. A strong correlation between *Shh* and *Cxcl12* expression patterns was observed. The loss of *Cxcl12* expression in the first branchial arch of *Smo*^{Wnt1Cre} embryos confirms the crucial role of the Hedgehog pathway for *Cxcl12* expression. However, activation of Hedgehog signaling had no effect on *Cxcl12* mRNA expression and *Cxcl12* promoter activity. Therefore, we propose that *Shh* may affect the expression pattern of *Cxcl12* by regulating the migration of *Cxcl12*$^{+}$ mesenchymal cells in the first branchial arch. Our data indicate that the expression of *Wnt5a* in the tongue is regulated by *Shh*, which is consistent with reports of hair follicle morphogenesis (Reddy et al., 2001). Several lines of evidence suggest that *Wnt5a* may mediate SHH signaling in the regulation of *Cxcl12*$^{+}$ mesenchymal cell migration. First, it is well documented that *Wnt5a* plays a crucial role in regulating cell migration and polarity (Yamaguchi et al., 1999). Second, expression of *Wnt5a* is lost in the tongue of *Isl1*^{ShhCre} embryos. Conversely, activation of SHH signaling in tissue explants can induce *Wnt5a* expression. Third, WNT5A attracts Cxcl12^{+} mesenchymal cells to migrate from the adjacent pharyngeal arch. Moreover, the attenuated defect in tongue morphogenesis and adequate restoration of myoblast invasion by expressing transgenic *Ihh* further strongly supports that Hedgehog signaling is required for tongue development. Based on these findings, we propose that *Isl1* regulates *Cxcl12*$^{+}$ mesenchymal cell migration through the SHH/WNT5A signaling cascade. Canonical Hedgehog signaling activation in NCCs is essential for the migration of *Cxcl12*$^{+}$ mesenchymal cells and myoblasts. In *Isl1*^{ShhCre} mutants, WNT5A in the proximal mesenchyme below *Shh*-expressing epithelium attracts *Cxcl12*$^{+}$ mesenchymal cells to cluster in the relatively small proximal region of the mandibular arch, resulting in a higher concentration of CXCL12 in this domain. The distal migration of *Cxcl12*$^{+}$ mesenchymal cells is essential for establishing a concentration gradient of CXCL12, which attracts myoblast invasion during tongue development.

Binding of CXCL12 to its receptor, CXCR4, triggers multiple intracellular signaling pathways related to chemotaxis (Chalasani et al., 2003; Ganju et al., 1998; Xu et al., 2010). Both tyrosine kinase and cyclic nucleotides have been reported to be essential for cell polarization and migration (Daaka et al., 1997; Guo and Cheng, 2015; Malherbe and Wang, 2012; Song et al., 1998). Our data suggest that the attractive effect of CXCL12 on myoblasts is mediated by the activity of tyrosine kinase, whereas cAMP is responsible for the repulsive effect of CXCL12 on myoblasts. It is possible that different concentrations of CXCL12 activate the distinct signal transduction pathways downstream of its receptor CXCR4, resulting in a ligand concentration-dependent bi-functional effect on myoblast invasion. In addition to regulation of migration processes, the CXCL12/CXCR4 signaling pathway promotes the growth and survival of different cells types (Molyneaux et al., 2003; Rubin et al., 2003; Sutton et al., 2007). Consistent with this, myoblast proliferation defects in myoblasts were detected in *Isl1*^{ShhCre} embryos at E11.5. The reduced cell proliferation could be due to the lack of interaction between *Cxcl12*$^{+}$ mesenchymal cells and *Cxcr4*$^{+}$ myoblasts in *Isl1*^{ShhCre} embryos. However, the differentiation process of the myoblasts was unaffected, suggesting that interaction between these two cells is required for myoblast proliferation rather than differentiation, which is consistent with previous findings that myoblast differentiation is not affected after CXCR4 inhibitor treatment (Griffin et al., 2010).

To the best of our knowledge, this is the first study to report that the ISL1/SHH/CXCL12 axis regulates *Cxcr4*$^{+}$ myoblast migration during tongue development. The concentration-dependent bidirectional regulation of CXCL12 on *Cxcr4*$^{+}$ myoblast migration and invasion may also be significant for the development of other organs, such as limbs. Our findings will promote the understanding of the mechanism of myoblast migration and open perspectives for studies of the pathogenesis of human tongue deformities and related syndromes.

MATERIALS AND METHODS

Animals

All animal procedures were approved by Hangzhou Normal University Animal Care and Use Committee (HNLA-2012-018). Construction of conditionally targeted *Isl1*^{fl} mice, *Isl1*^{lacZ} and Tg-*pmes-Ihh* conditional transgenic mice has been described previously (Elshatory et al., 2007; Li et al., 2017). *Shh*$^{tm1(EGFP/cre)}$, *Wnt1-Cre*, *Smo*$^{fl/fl}$ and *R26R-lacZ* were purchased from The Jackson Laboratory and maintained on a C57BL/6J background. The morning of observed vaginal plug was designated as day 0 (E0) of pregnancy.

SEM analysis

Embryos were fixed in 2.5% glutaraldehyde in 0.1 M phosphate buffer (pH 7.4) overnight. After rinsing in PBS, the sections were post-fixed with 1% osmium tetroxide solution for 1.5 h. Samples were dehydrated using a series of acetone solutions: 30%, 50%, 70%, 80%, 90%, 100% (three times)

Development (2022) 149, dev200788. doi:10.1242/dev.200788

for 15 min each. Samples were critically point-dried after a 15 min treatment with 95% isoamyl acetate. Samples were then mounted on conductive paper and sputter-coated with gold. Images were recorded with a scanning electron microscope (Hitachi S-3000N) with a 15-kV accelerating voltage.

X-gal staining

X-gal staining of whole-mount samples was performed as described previously (Li et al., 2017). Embryos were fixed in 4% paraformaldehyde (PFA) solution (with 5 mM EGTA and 2 mM $MgCl_2$) at 4°C for 1 h. The fixed embryos were rinsed three times in washing buffer (2 mM $MgCL_2$, 0.01% sodium deoxycholate and 0.02% NP-40 in PBS). The embryos were then incubated in staining solution (0.1% X-gal, 5 mM potassium ferricyanide, 5 mM potassium ferrocyanide, 2 mM Tris, pH 7.3, in washing buffer) overnight in the dark at 37°C. Lastly, the stained embryos were washed in PBS and used for whole-mount analysis. The X-gal-stained sections were counterstained with Nuclear Fast Red.

Quantitative real-time PCR

Total RNA from mouse mandibles was extracted from organ culture explants using TRIzol Reagent (Thermo Fisher Scientific). All RNA samples were treated with DNA-free DNA Removal Kit (Thermo Fisher Scientific). The first-strand complementary DNA (cDNA) was then synthesized from 1 µg of total RNA from each sample using a PrimeScript 1st Strand cDNA synthesis kit (Takara Bio). Quantitative RT-PCR was performed using the following primer sequences: *Isl1*, 5′-ATGATGGTGGTTTACAGGCTAAC and 5′-TCGATGCTACTTCACTGCCAG; *Shh*, 5′-AAAGCTGACCCCTTTAGCCTA and 5′-TGAGTTCCTTAAATCGTTCGGAG; *Ptch1*, 5′-AGACTACCCGAATATCCAGCACC and 5′-CCAGTCACTGTCAAATGCATCC; *Gli1*, 5′-CCAAGCCAACTTTATCAGGG and 5′-AGCCCGCTTCTTTGTTAATTTGA; *Foxd1*, 5′-AAAATCGCCCTATGCTGC and 5′-CTGGACCTGAGAATCTCTACACC; *Foxd2*, 5′-ATTTATGAAGAGTCTCCAGACC and 5′-GATGCTCAAACAGAAAAGC; *Foxf1*, 5′-ACTCCAGTGTCTTTCACCTTGC and 5′-TGAGCCTGAACTACACCAGC; *Foxf2*, 5′-TCAGTAGGACATTTCTTCC and 5′-CTGTCACAATACTGAGAGC; *Wnt5a*, 5′-CTAACAAGTGTGACAAGATCC and 5′-CTTGAAAGCAATGTCTAGC; *Cxcl12*, 5′-GACAGAAGAAGAGAAAGGCTGC and 5′-CCGAAGAGGGAAGAGTTTACC; *18S*, 5′-TAGAGGGACAAGTGGCGTTC and 5′-CGCTGAGCCAGTCAGTGT. The specificity for each primer set was confirmed by electrophoresis and sequencing before use. Real-time PCR experiments were performed in triplicate using SsoFast EvaGreen Supermix as previously described (Li et al., 2017). The relative amount of each gene transcript was calculated using the $2^{-\Delta\Delta CT}$ method and normalized to the endogenous reference gene *18S* (*Rn18s*). Data were analyzed with CFX Manager software and are represented as mean±s.e.m.

Immunohistochemistry and immunofluorescence

The collected embryos were fixed in 4% PFA solution, dehydrated, embedded in paraffin and sectioned as previously described (Li et al., 2019). Heat-induced epitope retrieval was used to unmask antigen epitopes (Li et al., 2019). For the cultured cells, 4% PFA solution was used for 10 min. After blocking in 1% bovine serum albumin (BSA), the sections were incubated with antibodies against MHC (1:20; Developmental Studies Hybridoma Bank), desmin (1:200; ab32362, Abcam), cyclin D1 (1:100; ab16663, Abcam), Pax3 (1:200; ab15717, Abcam), BrdU (1:100; ab6326, Abcam), CXCR4 (1:200; ab1670, Abcam) or Ki67 (1:200; ab15580, Abcam) at 4°C overnight. Then, horseradish peroxidase-conjugated secondary antibody against the primary antibody (1:200, sc-2004, Santa Cruz Biotechnology) was applied for 1 h at room temperature. For immunofluorescence, secondary antibodies conjugated with Alexa Fluor 488 or 594 (1:1000, Invitrogen) were used. Images were analyzed using a Leica DM4 B microscope equipped with a digital camera.

Histological analysis and *in situ* hybridization

Whole-mount and section *in situ* hybridization were performed as previously described (Li et al., 2017). For section *in situ* hybridization, samples were fixed in 4% PFA solution, dehydrated, embedded in paraffin and sectioned at 12 µm. For whole-mount *in situ* hybridization, samples were fixed in freshly made 4% PFA/PBS, dehydrated into methanol and bleached with 6% hydrogen peroxide (H_2O_2). Non-radioactive antisense RNA probes were generated by *in vitro* transcription using the DIG RNA labeling kit (Roche Diagnostics). For histological analysis, sections were stained with Hematoxylin and Eosin according to standard protocols.

Cell proliferation assay

Cell proliferation activity was evaluated by BrdU labeling and immunofluorescence staining. Timed pregnant mice were sacrificed 30 min after a single intraperitoneal injection of BrdU (Sigma-Aldrich) at 3 mg/100 g body weight. The collected embryos were fixed in 10% neutral buffered formalin at 4°C overnight and embedded in paraffin. BrdU-labeled cells were detected immunohistochemically on paraffin sections according to the manufacturer's instructions. The cell growth ratio (%) was calculated by dividing the number of BrdU-positive nuclei by the total number of nuclei.

Chemotaxis assay

The chemotactic response of mandible myoblasts to CXCL12 was evaluated using a 24-well fitted Transwell inserts with membranes (8 µm pore size, Corning Falcon). The inserts were then coated with Corning Matrigel matrix (Fisher Scientific) at 200 µg/ml. Mouse tongues were carefully dissected from E11 wild-type embryos. To remove the epithelium, the explants were incubated in 2.25% trypsin/0.75% pancreatin on ice for 5 min. One hundred microliters of isolated primary cells (mixture of myoblasts and mesenchymal cells) were added to the upper well of the chamber (2×10^5 per well). Both upper and lower chambers were loaded with Dulbecco's modified Eagle medium (DMEM) containing 1% fetal bovine serum (FBS). CXCL12 (R&D Systems) was used at concentrations of 0 ng/ml, 10 ng/ml, 100 ng/ml and 1000 ng/ml in the lower chambers of the Transwell. For the inhibitor treatment, cells were pretreated with 0.5 µg/ml AMD3100 (30 min at 37°C; A5602, Sigma-Aldrich), 1 µg/ml genistein (20 min at 37°C; 345834, Sigma-Aldrich) or 100 µM 8-Br-cAMP (15 min at room temperature; B7880, Sigma-Aldrich) before being added to the upper well of the chamber in selected experiments. For the competitive chemotaxis assay, CXCL12 (0, 10, 100 and 1000 ng/ml) was mixed with isolated primary cells (1×10^5 per well) plated to the upper chamber in media containing 1% (v/v) FBS. Media containing 3% (v/v) FBS was added to the lower chamber. The cells on the upper surface of the membrane were removed using a cotton swab after treatment for 24 h. The membranes were cut from inserts and mounted onto glass slides for immunofluorescence staining. The desmin antibody was used to label myoblasts. All experiments were repeated three to six times, and the number of invaded desmin$^+$ myoblasts was calculated.

Primary mesenchymal cell culture and luciferase assay

Mouse tongues were carefully dissected from E11 wild-type embryos. The explants were incubated in 2.25% trypsin/0.75% pancreatin on ice for 5 min to remove the epithelium. One hundred microliters of isolated primary mesenchymal cells were cultured in 24- or 96-well plates. The 2 kb promoter of *Cxcl12* was cloned into the pGL3 basic vector (pGL3-CXCL12 Pro) for the luciferase assay. The clone primer sequences were: 5′-CTAGCTCATCGTAGGAGGACC and 5′-CAGAGCTGGACAGCAAGAGG. The pGL3 empty vector (control) or pGL3-CXCL12 Pro vector was transfected with Lipofectamine3000 reagent. The next day, PUR (1 µM) or DMSO (control) was added to the culture media to activate the canonical Hedgehog signaling pathway. After incubation for 24 h in a humidified atmosphere of 5% CO_2 at 37°C, the cells were used for RNA isolation or luciferase activity analysis. Firefly luciferase activities were normalized to *Renilla* luciferase activity and each experiment was performed in triplicate at least three times.

In vitro organ culture and bead implantation

For bead-implantation experiments, mouse mandibles were carefully dissected from E10.5 wild-type embryos and placed into DMEM (Gibco) supplemented with 10% FCS. The explants were placed on a Nuclepore Track-Etch membrane (0.2-µm pore size) in Trowel-type organ culture dishes. WNT5A-saturated agarose beads (0.5 µg/µl),

CXCL12-saturated agarose beads (0.1 and 0.5 µg/µl) or SHH-saturated agarose beads (1 µg/µl) were grafted in the mandible. After being cultured for 16 h in a humidified atmosphere of 5% CO_2 at 37°C, the explants were fixed in 4% PFA overnight at 4°C, washed in PBS and finally stored in methanol at −20°C until analysis by whole-mount *in situ* hybridization. WNT5A, CXCL12 and SHH were purchased from R&D Systems. For *Isl1* overexpression experiments, the *Isl1* overexpression vector (pCDH-Isl1) or control vector (pCDH) was transfected with Lipofectamine3000 reagent. After being cultured for 48 h in a humidified atmosphere of 5% CO_2 at 37°C, the explants were used for RNA extraction and real-time PCR analysis.

Statistical analyses

All data are presented as mean±s.e.m. Unpaired, two-tailed Student's *t*-test was used to compare data sets. The threshold for statistical significance was $P<0.05$.

Acknowledgements

We thank Dr Lin Gan for providing *Isl1*^{fl} and *Isl1*^{lacZ} mice, and Dr Zunyi Zhang for comments and suggestions. We acknowledge the Center of Electron Microscopy of Zhejiang University for access to the scanning electron microscopes.

Competing interests

The authors declare no competing or financial interests.

Author contributions

Conceptualization: J. Liu, M.Q., F.L.; Methodology: J. Li, H.H., J. Liu, F.L.; Validation: J. Li, H.H., F.L.; Formal analysis: W.Z., J.Y., G.F., J. Li, F.L.; Investigation: W.Z., J.Y., F.L.; Resources: F.L.; Data curation: W.Z., J.Y., G.F., D.Y.; Writing - original draft: F.L.; Writing - review & editing: J. Li, H.H., J. Liu, D.Y., M.Q., F.L.; Visualization: W.Z., J.Y., G.F.; Supervision: F.L.; Project administration: F.L.; Funding acquisition: J. Li, D.Y., F.L.

Funding

This work was supported by grants from the National Natural Science Foundation of China (81871166 and 81670971 to F.L.) and Natural Science Foundation of Zhejiang Province (LY21C120002 to J.L., Y20C120004 to D.Y.).

Peer review history

The peer review history is available online at https://journals.biologists.com/dev/lookup/doi/10.1242/dev.200788.reviewer-comments.pdf.

References

Amano, O., Yamane, A., Shimada, M., Koshimizu, U., Nakamura, T. and Iseki, S. (2002). Hepatocyte growth factor is essential for migration of myogenic cells and promotes their proliferation during the early periods of tongue morphogenesis in mouse embryos. *Dev. Dyn.* **223**, 169-179. doi:10.1002/dvdy.1228

Belmadani, A., Tran, P. B., Ren, D., Assimacopoulos, S., Grove, E. A. and Miller, R. J. (2005). The chemokine stromal cell-derived factor-1 regulates the migration of sensory neuron progenitors. *J. Neurosci.* **25**, 3995-4003. doi:10.1523/JNEUROSCI.4631-04.2005

Bober, E., Franz, T., Arnold, H. H., Gruss, P. and Tremblay, P. (1994). Pax-3 is required for the development of limb muscles: a possible role for the migration of dermomyotomal muscle progenitor cells. *Development* **120**, 603-612. doi:10.1242/dev.120.3.603

Chai, Y. and Maxson, R. E.Jr. (2006). Recent advances in craniofacial morphogenesis. *Dev. Dyn.* **235**, 2353-2375. doi:10.1002/dvdy.20833

Chalasani, S. H., Sabelko, K. A., Sunshine, M. J., Littman, D. R. and Raper, J. A. (2003). A chemokine, SDF-1, reduces the effectiveness of multiple axonal repellents and is required for normal axon pathfinding. *J. Neurosci.* **23**, 1360-1371. doi:10.1523/JNEUROSCI.23-04-01360.2003

Cobourne, M. T., Iseki, S., Birjandi, A. A., Adel Al-Lami, H., Thauvin-Robinet, C., Xavier, G. M. and Liu, K. J. (2019). How to make a tongue: Cellular and molecular regulation of muscle and connective tissue formation during mammalian tongue development. *Semin. Cell Dev. Biol.* **91**, 45-54. doi:10.1016/j.semcdb.2018.04.016

Daaka, Y., Luttrell, L. M. and Lefkowitz, R. J. (1997). Switching of the coupling of the β2-adrenergic receptor to different G proteins by protein kinase A. *Nature* **390**, 88-91. doi:10.1038/36362

Doitsidou, M., Reichman-Fried, M., Stebler, J., Köprunner, M., Dörries, J., Meyer, D., Esguerra, C. V., Leung, T. C. and Raz, E. (2002). Guidance of primordial germ cell migration by the chemokine SDF-1. *Cell* **111**, 647-659. doi:10.1016/S0092-8674(02)01135-2

Elshatory, Y., Everhart, D., Deng, M., Xie, X., Barlow, R. B. and Gan, L. (2007). Islet-1 controls the differentiation of retinal bipolar and cholinergic amacrine cells. *J. Neurosci.* **27**, 12707-12720. doi:10.1523/JNEUROSCI.3951-07.2007

Ganju, R. K., Brubaker, S. A., Meyer, J., Dutt, P., Yang, Y., Qin, S., Newman, W. and Groopman, J. E. (1998). The alpha-chemokine, stromal cell-derived factor-1α, binds to the transmembrane G-protein-coupled CXCR-4 receptor and activates multiple signal transduction pathways. *J. Biol. Chem.* **273**, 23169-23175. doi:10.1074/jbc.273.36.23169

Griffin, C. A., Apponi, L. H., Long, K. K. and Pavlath, G. K. (2010). Chemokine expression and control of muscle cell migration during myogenesis. *J. Cell Sci.* **123**, 3052-3060. doi:10.1242/jcs.066241

Guo, C. L. and Cheng, P. L. (2015). Second messenger signaling for neuronal polarization: cell mechanics-dependent pattern formation. *Dev. Neurobiol.* **75**, 388-401. doi:10.1002/dneu.22217

He, F., Xiong, W., Yu, X., Espinoza-Lewis, R., Liu, C., Gu, S., Nishita, M., Suzuki, K., Yamada, G., Minami, Y. et al. (2008). Wnt5a regulates directional cell migration and cell proliferation via Ror2-mediated noncanonical pathway in mammalian palate development. *Development* **135**, 3871-3879. doi:10.1242/dev.025767

Jenkins, D. (2009). Hedgehog signalling: emerging evidence for non-canonical pathways. *Cell. Signal.* **21**, 1023-1034. doi:10.1016/j.cellsig.2009.01.033

Jeong, J., Mao, J., Tenzen, T., Kottmann, A. H. and McMahon, A. P. (2004). Hedgehog signaling in the neural crest cells regulates the patterning and growth of facial primordia. *Genes Dev.* **18**, 937-951. doi:10.1101/gad.1190304

Kaufman, M. H. and Bard, J. B. L. (1999). *The Anatomical Basis of Mouse Development*. San Diego: Academic Press.

Lewellis, S. W. and Knaut, H. (2012). Attractive guidance: how the chemokine SDF1/CXCL12 guides different cells to different locations. *Semin. Cell Dev. Biol.* **23**, 333-340. doi:10.1016/j.semcdb.2012.03.009

Li, F., Fu, G., Liu, Y., Miao, X., Li, Y., Yang, X., Zhang, X., Yu, D., Gan, L., Qiu, M. et al. (2017). ISLET1-dependent beta-Catenin/Hedgehog signaling is required for outgrowth of the lower jaw. *Mol. Cell. Biol.* **37**, e00590-16. doi:10.1128/MCB.00590-16

Li, J., Xu, J., Cui, Y., Wang, L., Wang, B., Wang, Q., Zhang, X., Qiu, M. and Zhang, Z. (2019). Mesenchymal Sufu regulates development of mandibular molars via Shh signaling. *J. Dent. Res.* **98**, 1348-1356. doi:10.1177/0022034519872679

Lin, C., Fisher, A. V., Yin, Y., Maruyama, T., Veith, G. M., Dhandha, M., Huang, G. J., Hsu, W. and Ma, L. (2011). The inductive role of Wnt-β-Catenin signaling in the formation of oral apparatus. *Dev. Biol.* **356**, 40-50. doi:10.1016/j.ydbio.2011.05.002

Liu, H.-X., Grosse, A. S., Iwatsuki, K., Mishina, Y., Gumucio, D. L. and Mistretta, C. M. (2012). Separate and distinctive roles for Wnt5a in tongue, lingual tissue and taste papilla development. *Dev. Biol.* **361**, 39-56. doi:10.1016/j.ydbio.2011.10.009

Lofqvist, A. and Lindblom, B. (1994). Speech motor control. *Curr. Opin. Neurobiol.* **4**, 823-826. doi:10.1016/0959-4388(94)90129-5

Ma, Q., Jones, D., Borghesani, P. R., Segal, R. A., Nagasawa, T., Kishimoto, T., Bronson, R. T. and Springer, T. A. (1998). Impaired B-lymphopoiesis, myelopoiesis, and derailed cerebellar neuron migration in CXCR4- and SDF-1-deficient mice. *Proc. Natl. Acad. Sci. USA* **95**, 9448-9453. doi:10.1073/pnas.95.16.9448

Mackenzie, S., Walsh, F. S. and Graham, A. (1998). Migration of hypoglossal myoblast precursors. *Dev. Dyn.* **213**, 349-358. doi:10.1002/(SICI)1097-0177(199812)213:4<349::AID-AJA1>3.0.CO;2-6

Malherbe, L. P. and Wang, D. (2012). Tyrosine kinases EnAbling adaptor molecules for chemokine-induced Rap1 activation in T cells. *Sci. Signal.* **5**, pe33. doi:10.1126/scisignal.2003383

Mayo, M. L., Bringas, P., Jr, Santos, V., Shum, L. and Slavkin, H. C. (1992). Desmin expression during early mouse tongue morphogenesis. *Int. J. Dev. Biol.* **36**, 255-263.

Melnick, M., Witcher, D., Bringas, P., Jr, Carlsson, P. and Jaskoll, T. (2005). Meckel's cartilage differentiation is dependent on hedgehog signaling. *Cells Tissues Organs* **179**, 146-157. doi:10.1159/000085950

Molyneaux, K. A., Zinszner, H., Kunwar, P. S., Schaible, K., Stebler, J., Sunshine, M. J., O'Brien, W., Raz, E., Littman, D., Wylie, C. et al. (2003). The chemokine SDF1/CXCL12 and its receptor CXCR4 regulate mouse germ cell migration and survival. *Development* **130**, 4279-4286. doi:10.1242/dev.00640

Noden, D. M. and Francis-West, P. (2006). The differentiation and morphogenesis of craniofacial muscles. *Dev. Dyn.* **235**, 1194-1218. doi:10.1002/dvdy.20697

Parada, C. and Chai, Y. (2015). Mandible and tongue development. *Curr. Top. Dev. Biol.* **115**, 31-58. doi:10.1016/bs.ctdb.2015.07.023

Parada, C., Han, D. and Chai, Y. (2012). Molecular and cellular regulatory mechanisms of tongue myogenesis. *J. Dent. Res.* **91**, 528-535. doi:10.1177/0022034511434055

Pfaff, S. L., Mendelsohn, M., Stewart, C. L., Edlund, T. and Jessell, T. M. (1996). Requirement for LIM homeobox gene Isl1 in motor neuron generation reveals a motor neuron-dependent step in interneuron differentiation. *Cell* **84**, 309-320. doi:10.1016/S0092-8674(00)80985-X

Poznansky, M. C., Olszak, I. T., Foxall, R., Evans, R. H., Luster, A. D. and Scadden, D. T. (2000). Active movement of T cells away from a chemokine. *Nat. Med.* **6**, 543-548. doi:10.1038/75022

Ratajczak, M. Z., Majka, M., Kucia, M., Drukala, J., Pietrzkowski, Z., Peiper, S. and Janowska-Wieczorek, A. (2003). Expression of functional CXCR4 by muscle satellite cells and secretion of SDF-1 by muscle-derived fibroblasts is associated with the presence of both muscle progenitors in bone marrow and hematopoietic stem/progenitor cells in muscles. *Stem Cells* **21**, 363-371. doi:10.1634/stemcells.21-3-363

Reddy, S., Andl, T., Bagasra, A., Lu, M. M., Epstein, D. J., Morrisey, E. E. and Millar, S. E. (2001). Characterization of Wnt gene expression in developing and postnatal hair follicles and identification of Wnt5a as a target of Sonic hedgehog in hair follicle morphogenesis. *Mech. Dev.* **107**, 69-82. doi:10.1016/S0925-4773(01)00452-X

Rubin, J. B., Kung, A. L., Klein, R. S., Chan, J. A., Sun, Y., Schmidt, K., Kieran, M. W., Luster, A. D. and Segal, R. A. (2003). A small-molecule antagonist of CXCR4 inhibits intracranial growth of primary brain tumors. *Proc. Natl. Acad. Sci. U.S.A.* **100**, 13513-13518. doi:10.1073/pnas.2235846100

Schlessinger, K., McManus, E. J. and Hall, A. (2007). Cdc42 and noncanonical Wnt signal transduction pathways cooperate to promote cell polarity. *J. Cell Biol.* **178**, 355-361. doi:10.1083/jcb.200701083

Song, H.-J., Ming, G.-L., He, Z., Lehmann, M., McKerracher, L., Tessier-Lavigne, M. and Poo, M.-M. (1998). Conversion of neuronal growth cone responses from repulsion to attraction by cyclic nucleotides. *Science* **281**, 1515-1518. doi:10.1126/science.281.5382.1515

Sutton, A., Friand, V., Brulé-Donneger, S., Chaigneau, T., Ziol, M., Sainte-Catherine, O., Poiré, A., Saffar, L., Kraemer, M., Vassy, J. et al. (2007). Stromal cell-derived factor-1/chemokine (C-X-C motif) ligand 12 stimulates human hepatoma cell growth, migration, and invasion. *Mol. Cancer Res.* **5**, 21-33. doi:10.1158/1541-7786.MCR-06-0103

Tajbakhsh, S. and Buckingham, M. (2000). The birth of muscle progenitor cells in the mouse: spatiotemporal considerations. *Curr. Top. Dev. Biol.* **48**, 225-268. doi:10.1016/S0070-2153(08)60758-9

Vasyutina, E., Stebler, J., Brand-Saberi, B., Schulz, S., Raz, E. and Birchmeier, C. (2005). CXCR4 and Gab1 cooperate to control the development of migrating muscle progenitor cells. *Genes Dev.* **19**, 2187-2198. doi:10.1101/gad.346205

Witze, E. S., Litman, E. S., Argast, G. M., Moon, R. T. and Ahn, N. G. (2008). Wnt5a control of cell polarity and directional movement by polarized redistribution of adhesion receptors. *Science* **320**, 365-369. doi:10.1126/science.1151250

Xu, H., Leinwand, S. G., Dell, A. L., Fried-Cassorla, E. and Raper, J. A. (2010). The calmodulin-stimulated adenylate cyclase ADCY8 sets the sensitivity of zebrafish retinal axons to midline repellents and is required for normal midline crossing. *J. Neurosci.* **30**, 7423-7433. doi:10.1523/JNEUROSCI.0699-10.2010

Yamaguchi, T. P., Bradley, A., McMahon, A. P. and Jones, S. (1999). A Wnt5a pathway underlies outgrowth of multiple structures in the vertebrate embryo. *Development* **126**, 1211-1223. doi:10.1242/dev.126.6.1211

Yang, L., Cai, C.-L., Lin, L., Qyang, Y., Chung, C., Monteiro, R. M., Mummery, C. L., Fishman, G. I., Cogen, A. and Evans, S. (2006). Isl1Cre reveals a common Bmp pathway in heart and limb development. *Development* **133**, 1575-1585. doi:10.1242/dev.02322

Ziermann, J. M., Diogo, R. and Noden, D. M. (2018). Neural crest and the patterning of vertebrate craniofacial muscles. *Genesis* **56**, e23097. doi:10.1002/dvg.23097

Zou, Y.-R., Kottmann, A. H., Kuroda, M., Taniuchi, I. and Littman, D. R. (1998). Function of the chemokine receptor CXCR4 in haematopoiesis and in cerebellar development. *Nature* **393**, 595-599. doi:10.1038/31269